

## ON THE POSSIBILITY OF REALIZING SHORTEST BUNCHES IN LOW-ENERGY STORAGE RINGS

*A. Papash*<sup>a,d</sup>, *C. P. Welsch*<sup>a-c</sup>

<sup>a</sup> Max Planck Institute for Nuclear Physics, Heidelberg, Germany

<sup>b</sup> Kirchhoff Institute for Nuclear Physics, University of Heidelberg, Heidelberg, Germany

<sup>c</sup> Gesellschaft für Schwerionenforschung, Darmstadt, Germany

<sup>d</sup> Joint Institute for Nuclear Research, Dubna

For some very interesting experiments in future low-energy storage rings it is highly desirable to realize ultrashort bunches in the nanosecond regime. These bunches could then be used for collision studies with atomic or molecular gas jet targets where the time structure of the bunches would be used as a trigger for the experiment. Thus, the control of the longitudinal time structure of the stored beam is of central importance since it directly determines the quality of the envisaged experiments. Over many years, it has been a significant challenge for the storage ring accelerator physics community to develop techniques to reduce the duration of bunches. Up to now, all methods that have been developed go along with various difficulties, which can include reduced stored-beam lifetimes. Thus, novel and innovative concepts for the manipulation and control of the longitudinal beam structure will have to be developed. In this paper, a possible approach to realize shortest bunches in an electrostatic storage ring is presented.

Для проведения некоторых перспективных ядерно-физических экспериментов на накопительных кольцах низких энергий необходимо получать сгустки частиц длительностью порядка 1–2 нс. Ультракороткие импульсы ускоренных ионов могут быть использованы для исследования реакций соударения частиц пучка с атомами, а также молекулами газовой мишени. Импульсная структура пучка позволяет применять сгустки ионов в качестве триггера для начала отсчета эксперимента. Формирование и контроль временной структуры накопленного пучка имеют принципиальное значение, так как длительность сгустка определяет качество проводимых исследований. Эксперименты по уменьшению длины сгустков в накопительных кольцах проводятся на протяжении многих лет и часто сопровождаются сокращением времени жизни пучка, а также другими побочными эффектами. Необходимо разрабатывать новые, нестандартные методы для контроля параметров пучка в продольном фазовом пространстве. В статье обсуждается одна из возможностей реализации ультракоротких сгустков для накопителей низких энергий.

PACS: 29.20.Ba; 29.20.-D; 41.75.-i; 41.85.-p

### INTRODUCTION

Low-energy antiprotons are the ideal and perhaps the only tool to study in detail correlated quantum dynamics of few-electron systems in the femto- and sub-femtosecond time regime. Unfortunately, cooled beams of antiprotons with the necessary beam quality and luminosity are not yet available and cannot be provided with present scientific infrastructures. In order to pave the way for a next-generation low-energy antiproton facility, challenging developments

in both, storing and imaging techniques have been launched at MPI-K. A novel ultralow energy storage ring (USR) [1, 2] to be integrated at the proposed facility for low-energy antiproton and ion research (FLAIR) [3, 4] is being developed to provide electron-cooled beams of antiprotons and possibly highly charged ions in the energy range between 300 and 20 keV, maybe even approaching the sub-keV regime.

To allow for kinematically complete investigations for a variety of collision processes, a reaction microscope shall be integrated in the ring, thus achieving unprecedented luminosities [5, 6]. For these collision experiments, around  $10^4$  antiprotons are required per bunch. This number is well below the space charge limit of the USR even at the lowest energies. However, the time structure of the pulses needs to be in the order of a few nanoseconds to allow its use as a trigger signal for the measurements. In this respect, an efficient control of the longitudinal time structure of the stored ion beam is of central importance since it directly determines the quality of the envisaged experiments.

The reason why ultrashort pulses in the nanosecond regime are extremely hard to realize is partially the strong space charge limitations that were found in existing electrostatic machines, probably linked to nonlinear fields that cannot be avoided in such storage rings. The nature of these effects is not yet understood and it is a part of ongoing studies in the QUASAR group at MPI-K to simulate the motion of a stored ion beam in an electrostatic cooler synchrotron under consideration of nonlinear fields as well as space charge effects, together with a particular focus on the needs of both internal and external experiments.

## **GENERAL APPROACH TO SHORT PULSES OPERATION**

It is technically possible to provide ultrashort pulses of 20 keV antiprotons by manipulation of the time structure of an extracted beam. The combination of an RF cavity operating at a higher harmonics of the ion rotation frequency and a fast extraction provided by a pulsed deflector would produce bunches of 50 to 100 ns duration. By employing the well-established technique of low-energy beam bunching and by installation of a phase compressor (or a few phase rotators) in the beam line, one may envisage to produce desirable bunches of pulse width with a few nanoseconds duration. These pulses could then be delivered to some remote experimental area.

The disadvantage of the above-mentioned scheme, however, is that the beam will interact with the gas jet only once per cycle and thus a sufficient luminosity as required by the experiments could not be reached. In this paper we thus consider the possibility of producing ultrashort pulses of a beam circulating in the ring. Taking into account the present USR layout (which is not yet finalized), one has to admit that it is impossible to create ultrashort bunches of a few nanoseconds duration directly from a circulating coasting beam at an energy of only 20 keV. The required buncher voltage to provide a 2 ns time focus from a coasting beam, where the revolution period at 20 keV in the USR is  $\tau \sim 20 \mu\text{s}$ , would exceed 10 kV and thus the induced energy spread by the phase compression would simply destroy the beam circulating in the ring.

Nevertheless, an operation with ultrashort pulses for in-ring experiments might still be realized by applying the following sequence of procedures:

After the beam has been slowed down to an energy of 20 keV, the coasting beam of antiprotons is cooled down to a momentum spread of  $\sim 5 \cdot 10^{-4}$ . The cooling time to reach

the equilibrium stage was estimated by the BETACOOOL code and should not exceed 1.5 s [7]. The required voltage to decelerate the beam from 300 to 20 keV in about less than a second will be smaller than 10 V and a drift tube is foreseen to slow down the ions.

After the cooling process, the coasting beam is adiabatically captured into  $\tau \sim 50$  ns stationary buckets formed by a 20 MHz cavity operating at a high harmonic mode of the ring revolution frequency ( $h_{\text{RF}} = 300\text{--}400$ ). The repetition rate of the bunches is thus 20 MHz and the distance between pulses is 50 ns. The final pulse width of a bunch will depend on the initial RF voltage applied to capture the circulating beam.

The desired ultrashort pulses of 1–2 ns duration are then formed by an additional  $3\beta\lambda/2$  double drift buncher with a relatively low voltage. It should be pointed out that using any kind of RF device to provide phase compression will automatically lead to an additional energy spread, which will lower the experimental resolution. Thus, any manipulation of short pulses must be limited to the straight sections of the ring where the dispersion function is zero.

Once the experimental section is crossed, bunch rotation to provide phase decompression will be mandatory. Otherwise the growing energy spread introduced by the phase compressor will cause a beam blowup in the bending sections of the USR due to an unavoidable coupling of motion in longitudinal and transverse phase spaces in an electrostatic cylinder deflector.

In the present scheme the buncher for phase compression is located at the beginning of one of the straight sections of the USR, downstream of a bending deflector. As pointed out before, the dispersion function is equal to zero in the straight sections of this storage ring. The buncher should provide a time focus with a width of about 1 ns in the symmetry point of the straight section where the reaction microscope is located. An RF phase decompressor is then to be located downstream of the reaction microscope. The bunch rotator should partly compensate an energy spread introduced by the phase compression buncher and thus limit the growth of the equilibrium momentum spread to an acceptable level.

Some crucial questions have to be answered before any detailed analysis of the pulsed mode can be done:

1. What are the pulse structure and main parameters of the low-energy buncher, including its voltage, gaps, tube diameter?
2. What is the RF frequency range for short pulses production?
3. What is the optimum location of the buncher and debuncher?
4. What are the parameters of the RF cavity in order to ensure an operation at a higher harmonics while maintaining a proper separatrix area for a beam with growing energy spread?
5. What modifications to the present ring structure will be required to accommodate the beam pulsing system?

The original layout of the USR foresaw  $90^\circ$  bending elements in each of the ring's corner sections (Fig. 1) [3, 8] while a modified design as shown in Fig. 2 was proposed in 2006 [1]. This layout, however, is still under consideration and will ultimately depend on the experiments that are envisaged by the wider physics community.

In this paper, we consider the original layout of the machine as well as a slightly modified layout of the machine, where the bending section in the corners is split up into two  $8^\circ$  deflectors and one  $74^\circ$  deflector. The ring parameters with emphasis on the short pulse operation mode are presented in Table 1. In this table, the beam parameters at 300 keV

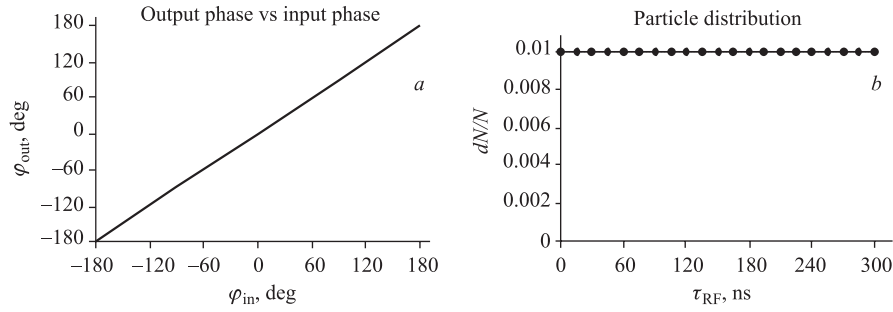


Fig. 1. Buncher\_U400 code output with zero voltage on the buncher. *a)*  $\varphi_{\text{out}}$  as a function of  $\varphi_{\text{in}}$ ; *b)* intensity distribution vs RF phase:  $dN/N = f(\varphi_{\text{in}})$

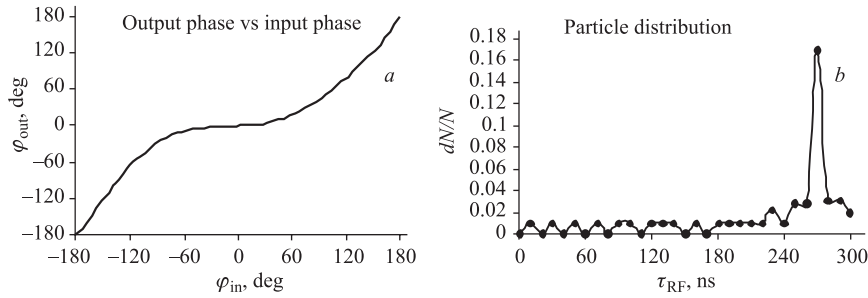


Fig. 2. Beam pulses at an RF frequency of 1 MHz. The drift length between buncher and the reaction microscope is assumed to be  $L_{\text{drift}} = 2$  m,  $V = 5.6$  kV. Pulse width is  $\tau \sim 15$  ns

Table 1. Parameters of Ultralow Storage Ring related to short pulse operation mode

| Parameter   | 90° deflector                         |                      | 8° + 74° + 8° deflector               |                      |
|---|---------------------------------------|----------------------|---------------------------------------|----------------------|
|   | Injection                             | Extraction           | Injection                             | Extraction           |
| Energy $E$ , keV  | 300                                   | 20                   | 300                                   | 20                   |
| Ring circumference $L$ , m                                  | 34.96                                 |                      | 42.984                                |                      |
| $\beta = v/c$   | $2.53 \cdot 10^{-2}$                  | $6.53 \cdot 10^{-3}$ | $2.53 \cdot 10^{-2}$                  | $6.53 \cdot 10^{-3}$ |
| Rotation period $T = L/\beta c$ , $\mu\text{s}$             | 4.609                                 | 17.858               | 5.667                                 | 21.957               |
| Rotation frequency, $F_{\text{rot}} = 1/T$ , kHz            | 216.9                                 | 55.997               | 176.46                                | 45.5436              |
| RF cavity frequency $F_{\text{RF}}$ , MHz                   | 20.1717                               | 20.15892             | 20.1164                               | 20.0392              |
| RF harmonic number $h_{\text{RF}}$                          | 93                                    | 360                  | 114                                   | 440                  |
| Bucket RF width, $\tau = 1/F_{\text{RF}}$ , ns              | 49.57                                 | 49.6                 | 49.71                                 | 49.9                 |
| Buncher drift space, cm                                     | 200                                   | 200                  | 200                                   | 200                  |
| Optimum buncher voltage, V                                  | 21,500                                | 370                  | 21,500                                | 370                  |
| Buncher frequency $F_{\text{RF}}$ , MHz                     | 20.1717                               | 20.15892             | 20.1164                               | 20.0392              |
| Expected pulse width, ns                                    | 1–2                                   | 1–2                  | 1–2                                   | 1–2                  |
| Momentum spread (before e-cooling / after e-cooling) $dP/P$ | $5 \cdot 10^{-3}$ / $5 \cdot 10^{-4}$ | $5 \cdot 10^{-4}$    | $5 \cdot 10^{-3}$ / $5 \cdot 10^{-4}$ | $5 \cdot 10^{-4}$    |

End of Table 1

| Parameter   | 90° deflector |                                      | 8° + 74° + 8° deflector |                                       |
|---|---------------|--------------------------------------|-------------------------|---------------------------------------|
|   | Injection     | Extraction                           | Injection               | Extraction                            |
| Maximum dispersion $D_{\max}$ , m   | 2             | 2                                    | 2                       | 2                                     |
| Gap between deflector plates, cm  | $\pm 6$       | $\pm 6$                              | $\pm 6$                 | $\pm 6$                               |
| Max. allowed momentum spread $dP/P$ , %   | $\pm 3$       | $\pm 3$                              | $\pm 3$                 | $\pm 3$                               |
| Transition factor $\gamma_{\text{tr}} \approx \nu_R$  |               | 2.2                                  |                         | 2.2                                   |
| Momentum compaction $\alpha \approx (\gamma_{\text{tr}})^{-2}$  |               | 0.207                                |                         | 0.207                                 |
| Frequency slip factor $\eta = (\gamma_{\text{tr}})^{-2} - (\gamma)^{-2}$                                  |               | -0.8                                 |                         | -0.8                                  |
| Synchrotron frequency $\Omega_S$ , kHz,<br>with $eV_{\text{RF}}$ in volts                                 |               | $1.88 \times (eV_{\text{RF}})^{1/2}$ |                         | $1.707 \times (eV_{\text{RF}})^{1/2}$ |
| Average radius $R_{\text{av}}$ , m  | 5.588         |                                      | 6.83                    |                                       |
| Infinity frequency $\omega_{\infty} = c/R_{\text{av}}$ , MHz  | 53.65         |                                      | 43.89                   |                                       |
| Range of RF cavity voltage change, V  |               | 10–2000                              |                         | 10–2000                               |
| Momentum $pc$ , MeV   | 23.72         | 6.12                                 | 23.72                   | 6.12                                  |
| Magnetic rigidity $BR$ , T·m  | 0.07908       | 0.0204                               | 0.07908                 | 0.0204                                |
| Time of flight in the region of electric<br>field of buncher, $\tau_{\text{eff}} = X_{\text{gap}}\beta c$ |               |                                      |                         |                                       |
| $\tau_{\text{eff}}$ , ns (RF, °) (eff. gap $X_{\text{eff}} = 20$ mm)                                      | 2.6 (19)      | 10 (70)                              | 2.6 (19)                | 10 (70)                               |
| $\tau_{\text{eff}}$ , ns (RF, °) (eff. gap $X_{\text{eff}} = 35$ mm)                                      | 4.7 (34)      | 18 (130)                             | 4.7 (34)                | 18 (130)                              |
| $\beta$ function at the buncher location, m   |               | 10                                   |                         | 10                                    |
| $D$ dispersion at the buncher location, m   |               | 0                                    |                         | 0                                     |
| Expected beam size at buncher position, mm<br>(for an emittance of $5\pi$ mm-mrad)                        |               | 14                                   |                         | 14                                    |

injection energy and 20 keV extraction energy are compared for two different geometries of ring. The RF phase gymnastics is expected to be applied to the antiproton beam at lowest energies, i.e., at 20 keV. Similar estimations can be done for a variety of ions and for different energy ranges.

**Choice of Parameters for Low-Energy Phase Compressor.** The estimations of the parameters of the USSR phase compressor as well as the expected pulse structure of beam shown in this paper are based on the computer code *Buncher\_U400* which is typically used to simulate the beam parameters in an accelerator injection line [9]. Since a commonly used injection energy is in the range between 20 and 30 keV, one should not expect fundamental differences between a DC beam in an injector and the coasting beam in a storage ring. Bunchers for different injection lines were successfully designed with the help of the above-mentioned code and are in operation in many accelerators and show good agreement with the computer simulations.

In its standard operation mode with a DC beam, either a single buncher or a combination of two bunchers operating at the first and second harmonics of the main RF is used to modulate the beam density into nodes. For instance, in a standard axial injection line of a cyclotron, up to 70% of the beam intensity is being compressed into bunches of desired pulse width, while the rest of beam is considered as «tails».

In the present study, we applied a sinusoidal voltage of 20 MHz frequency to the phase compressor and assumed that the beam has already been bunched to 25 ns pulses by adiabatic capture into RF buckets. The phase expansion of each bunch is thus  $\pi$  out of a full bucket width of  $2\pi$ . In other terms, we assume that the beam pulses of 25 ns duration each fly

through the RF compressor every 50 ns. Thus, 50 ns beam bunches following every 100 ns correspond to a repetition frequency of 10 MHz, while pulses of 12.5 ns width correspond to a 40 MHz repetition rate. Clearly, beam losses caused by the bunch compression have to be carefully estimated. In the framework of this study we assumed that the main RF cavity will keep the beam captured in the buckets and that the ion losses after the phase compressor(s) will be reasonably small.

The code is able to consider the gap crossing effect, influences from the space charge, as well as either a linear or a sinusoidal shape of the RF wave. The equations of motion are treated with the independent variable  $\tau$  (RF time) in the gap region between the buncher electrodes (in solid edge approximation), while outside the buncher the particle motion is treated by an analytic description. Thus, by an adequate choice of the buncher gap one may estimate the effect from the electrode fringe fields.

We studied the particle motion in 1D space in energy–phase coordinates  $(E, \varphi)$  assuming no coupling between the transverse and longitudinal motion. The  $2\pi$  phase band is divided into a number of intervals corresponding to a specific certain RF phase  $\varphi_i$  with an RF voltage amplitude proportional to  $\sin(\varphi_i)$ . In each interval, we entered a specific number of particles. The beam density distribution is then calculated as the relative number of particles in each interval after crossing the drift distance between the buncher and its time focus.

The results from the calculations when the buncher is off are presented in Fig. 1.

One may see that the variation of the output phase is linear with respect to the input phase and that the distribution of the beam current density is homogeneous. In the program, the input phases as well as output phases are varied from  $-180^\circ$  to  $+180^\circ$ . This simply means that there is no modulation of the beam density when the buncher is off.

In a second step, a 1 MHz RF voltage is applied to the beam bunches which were previously compressed to 500 ns pulses. In principle this should allow for providing a timing focus at a distance of 2 m downstream of the compressor. However, as can be seen in Fig. 2, the minimum available pulse width at the position of the reaction microscope will be at least 15 ns and the required amplitude of the buncher voltage exceeds 5–6 kV. The resulting energy spread caused by a 1 MHz phase compressor would thus lead to immediate loss of the beam in the dispersion sections of the ring.

Increasing the RF frequency to 10 MHz, bunches with a pulse width of 2 ns become available in its time focus at the position of the reaction microscope, Fig. 3. In this case, a voltage of  $V_{\text{bunch}} = 715$  V needs to be applied.

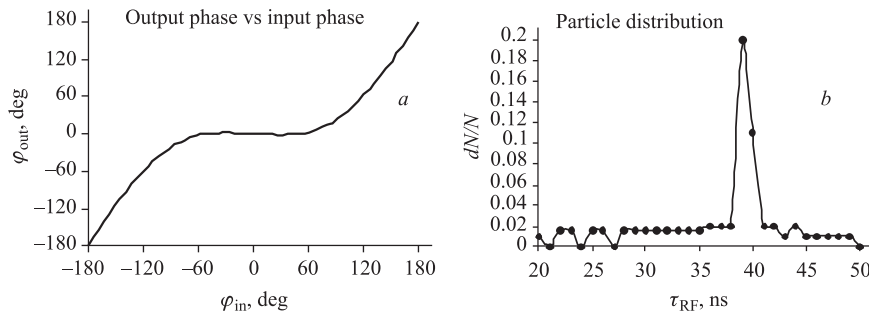


Fig. 3. Beam pulses at an RF frequency of  $f_{\text{RF}} = 10$  MHz. The buncher voltage of 715 V was selected to focus the beam on the reaction microscope. The minimum available pulse width is  $\tau = 2$  ns

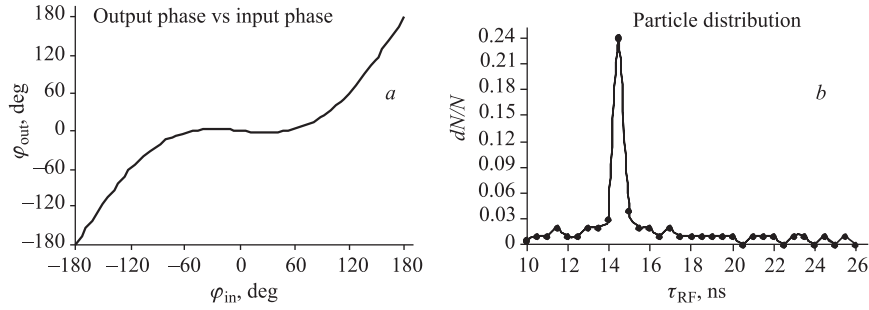


Fig. 4. Beam pulses at an RF frequency of  $f_{\text{RF}} = 20$  MHz. The amplitude of the buncher voltage is  $V = 515$  V and is optimized to focus the beam pulse on the reaction microscope after a drift of  $L_{\text{drift}} = 1.4$  m. The width of the gap is  $d_{\text{gap}} = 20$  mm and the pulse width is  $\tau = 1$  ns

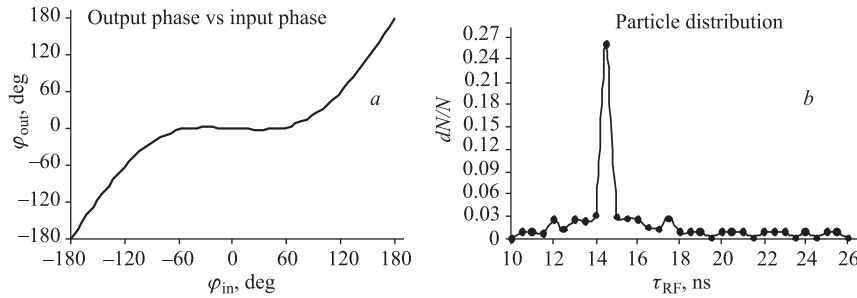


Fig. 5. Beam pulses at an RF frequency of  $f_{\text{RF}} = 20$  MHz. The amplitude of the buncher voltage is  $V = 370$  V and is optimized to focus the beam pulse on the reaction microscope after a drift of  $L_{\text{drift}} = 2.0$  m. The width of the gap is  $d_{\text{gap}} = 20$  mm and the pulse width is  $\tau = 1$  ns

Finally a buncher operating at 20 MHz RF frequency is able to compress 20–30 ns bunches to 1 ns pulses, see Figs. 4 and 5, which is in line with the desired pulse duration. It should be noted that a further increase of the compressor RF frequency range would cause time-of-flight effects during the passage of the electric field region in the buncher. For that reason an RF frequency of  $f_{\text{RF}} = 20$  MHz was selected for all further considerations as the optimum.

We would like to remind the reader that the preliminary design of the USR included straight sections only 2.8 m in length, while for an installation of a merged positron beam one would need 4 m long straight sections, which is why we considered both cases in our present study.

From the results in Figs. 4 and 5 one can see that a voltage of 370 V is required to provide a time focus of the 20 keV beam at the symmetry point of a «long» straight section ( $L_{\text{drift}} = 2$  m), while this voltage needs to be increased to 515 V in case only a shorter distance is available. With the aim to minimize the energy spread produced by the buncher, it is thus preferable to keep the straight section at 4 m, therefore keeping the option of including even larger experimental installations in the USR.

At this point it should also be noted that our calculations clearly indicated that the use of this phase gymnastics method would be impossible at a beam energy of  $E = 300$  keV. Even for a drift length of 2 m, the amplitude of buncher voltage would have to be 21.5 kV.

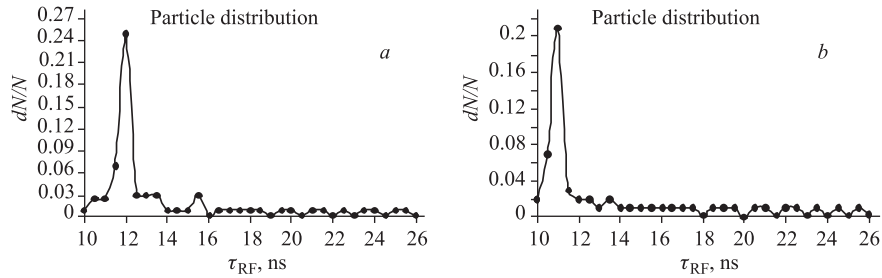


Fig. 6. Assumed effective field length of 25 mm (a) and 30 mm (b) at  $f_{RF} = 20$  MHz. Buncher voltages are 390 and 380 V, respectively, with  $L_{drift} = 2.0$  m and a pulse duration of a least 1.5 ns

Because of the low beam energy, time-of-flight effects during the passage of the electric field region between the buncher electrodes are of great importance especially for high RF frequency operation. The effective length of the electric field in the buncher might be approximated by the expression  $d_{el.flid} = d + R_1 + R_2$ , where  $d$  is geometric distance between the electrodes, and  $R_1$  and  $R_2$  are the aperture radii of the first and second electrodes. Since the required amplitude of the RF voltage is less than 400 V, the gap between the electrodes might be safely reduced to around 3 mm. For a double gap drift buncher it should be feasible to use voltages of up to 500 V between the different electrodes even for small spacings. The minimum drift tube aperture is determined by the beam size before the cooling process. Assuming an initial emittance of  $\varepsilon = 5$  mm · mrad, a beta function at the buncher location of  $\beta = 10$  m and a dispersion in the straight section of  $D = 0$ , the maximum beam diameter should not exceed 14 mm. This means that the effective length of the electric field  $d_{el.flid}$  in the buncher will be larger than 17 mm.

While the beam pulse width for a distance of  $d_{el.flid} = 20$  mm was shown in Fig. 5, the cases where  $d_{el.flid} = 25$  mm and  $d_{el.flid} = 30$  mm are shown in Fig. 6. In these cases, the shortest available pulse width would be around 1.5 ns, which is 50% higher than the target value.

At even larger gap distances, there is no bunching effect at all when the effective field length exceeds  $d_{el.flid} = 35$  mm. In this case, the time of flight between the drift tubes is almost 18 ns, thus corresponding to roughly  $150^\circ$  in RF phase.

Taking into account expected beam size at the buncher location, the minimum drift tube aperture cannot be reduced to less than 17–22 mm. Thus, the effective gap extension is  $d_{el.flid} = 20$ –25 mm and thus employing an RF frequency higher than 20 MHz is not feasible due to fringe field effects.

**Pulse Width of Beam with Momentum Spread.** The phase compression was also investigated for a beam with a given energy spread. Simulations were done with a well-defined deviation from the design beam energy 20 keV, while keeping the same amplitude of the buncher voltage as for the design energy. Particles with a large momentum spread of up to  $dp/p = \pm 4\%$  were traced through buncher tuned for nominal beam energy.

In this case the pulse width slightly increased from an initial value of 2 to 2.2 ns when  $dp/p$  varies between  $-0.15\%$  and  $-4\%$ , see Fig. 7. It was found that the pulse width does not change for a momentum deviation of up to  $dp/p = 2\%$ , and increased from 1.3 to 1.7 ns when the momentum spread grows from  $+2.5\%$  to  $+4\%$ , Fig. 8.



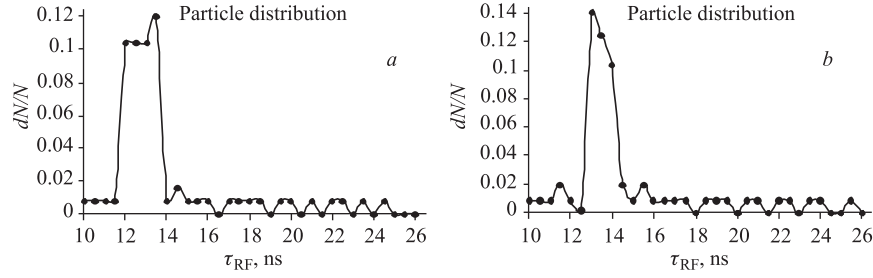


Fig. 7. Bunching of beam with momentum deviation of  $dp/p = -4\%$  (a) and  $dp/p = -0.15\%$  (b). Pulse width is 2.2 and 2 ns, respectively

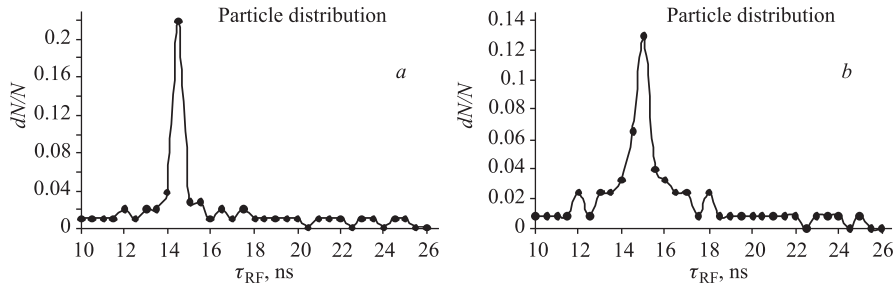


Fig. 8. Bunching of beam with momentum deviation of  $dp/p = 2.5\%$  (a) and  $dp/p = 4\%$  (b). Pulse width is 1.3 and 1.7 ns, respectively

It should be noted in this context, that the maximum value of the ring dispersion function does not exceed  $D = 2$  m in the middle of the large bending deflector. In order to be able to accommodate even beams with large energy spread, we enlarged the gap between the deflector plates to 12 cm. In this case, it is possible to keep particles with a momentum spread of up to  $\pm 2\%$  on a stable orbit.

### ESTIMATION OF ENERGY COMPRESSOR (DEBUNCHER) PARAMETERS

In the previous section, we estimated the parameters of the phase compressor. The evolution of a beam bunch is shown schematically in Fig. 9. In order to provide a time focus at a distance of  $L_{\text{drift}} = 2$  m downstream of the buncher, the required amplitude of the phase compressor voltage should be  $V_{\text{bunch}} = 370$  V.

Bunches of 1–2 ns pulse width are then produced in the middle of the storage rings' straight section.

In order to estimate the longitudinal emittance of a coasting beam in the ring, one may use the following formula:

$$\varepsilon_{\text{long}\Sigma} = \pi \Delta E T_0, \quad (1)$$

where  $\Delta E$  is the energy spread and  $T_0$  is the revolution time of ions in the ring. The energy spread of the unbunched beam *before cooling* is expected to be around  $\Delta E/E = 5 \cdot 10^{-3}$  at an energy of  $E = 20$  keV. The longitudinal emittance of the coasting beam before cooling is then equal to  $\varepsilon_{\text{long}\Sigma} \approx 100 T_0$ , i.e.,  $\varepsilon_{\text{long}\Sigma} = (1780-2200) \pi$  keV · ns.

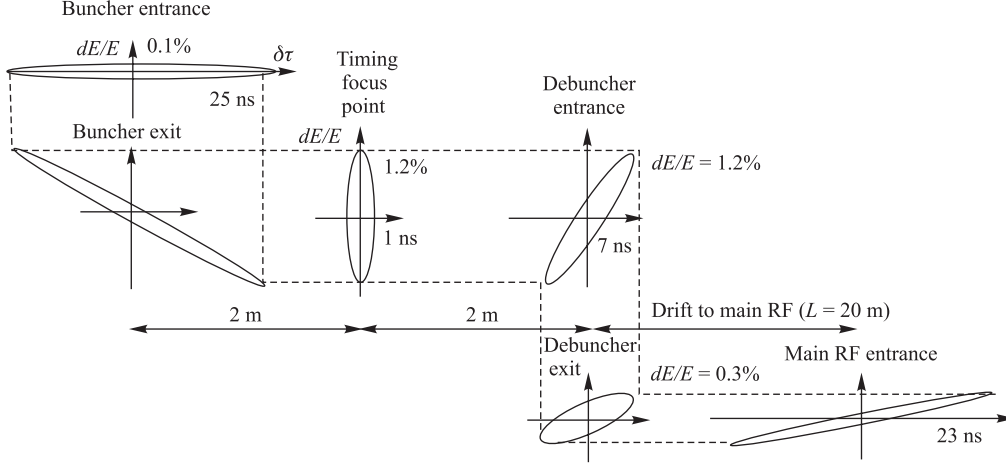


Fig. 9. Sketch of the evolution of the phase space ellipses in the short pulse operation mode

The equilibrium energy spread of the coasting beam after cooling is expected to be no more than  $\Delta E/E = 5 \cdot 10^{-4}$  [7]. Thus, in this case the longitudinal emittance of the cooled beam is estimated to  $\varepsilon_{\text{long}\Sigma} \approx 10 T_0$ , i.e.,  $\varepsilon_{\text{long}\Sigma} = (178-220) \pi \text{ keV} \cdot \text{ns}$ .

The minimum voltage required to fully bunch a debunched beam of the total area  $\varepsilon_{L\Sigma} = \Delta E T_0$  is

$$eV = \frac{\pi \varepsilon_{\text{lt}}^2 h |\eta|}{128 (R/c)^2 E}. \quad (2)$$

The RF voltage which has to be applied to the USSR RF cavity to fully capture the uncooled coasting beam is between 70 and 80 V and is in the order of 1 V to capture the beam that has been cooled down to the equilibrium condition.

Taking into account only the main RF cavity, operating at 20 MHz, the coasting beam is adiabatically captured into buckets of 50 ns pulse width. The area of each bunch in the longitudinal phase space can then be estimated as  $\varepsilon_{\text{lb}} = \pi 20 \text{ eV} \cdot 25 \text{ ns} = 0.5\pi \text{ keV} \cdot \text{ns}$ , with  $\Delta E/E = 10^{-3}$ .

Assuming the conservation of the longitudinal emittance after the passage of the phase compressor, one may estimate the energy spread increase caused by the bunching process. In the time focus where the shortest pulse width should be  $\Delta\tau = 2 \text{ ns}$  (upright position of the phase ellipse), the phase width of the bunch is  $14^\circ$  RF for 20 MHz and the corresponding energy spread is  $\Delta E = \varepsilon_{\text{lb}}/\Delta\tau = 0.25 \text{ keV}$ . The relative energy spread after the phase compressor was estimated as  $\Delta E/E \sim 1.2 \cdot 10^{-2}$ . The ideal distance to install the debuncher could then be calculated from the following formula:

$$L_{\text{opt}} = \frac{(\beta\lambda) (\Delta\varphi/\pi)}{(\Delta E/E)}, \quad (3)$$

where  $\Delta\varphi$  is phase advance of the particles after the time focus,  $\beta$  the relativistic factor and  $\lambda$  the wave length of the RF.

In order to minimize the energy spread after the buncher and to fully exploit the decompressing technique by using a sine wave debuncher, one should locate the phase decompressor at a distance where the phase ellipse in longitudinal phase space is rotated by  $45^\circ$  from the time focus, see Fig. 9. At this position the linear part of the sine wave voltage is fully used. The optimum drift distance  $L_{\text{opt}}$  to place the debuncher can directly be derived from (3):

$$L_{\text{opt}} = \frac{(\beta\lambda/4)}{(\Delta E/E)} = \frac{300\beta/4f_{\text{RF}}}{\Delta E/E} \quad [\text{m, MHz}]. \quad (4)$$

For the particular case of an energy spread of  $\Delta E/E = 1.2\%$ , the optimum position of the debuncher should be at a distance of  $L_{\text{opt}} = 1.95$  m from the time focus. Thus, the optimum distance from the middle of the straight section to the phase debuncher is  $L_{\text{opt}} = 4.8$  m if the energy spread after the buncher is  $\Delta E/E = 5 \cdot 10^{-3}$ .

Clearly it is best to provide this «phase gymnastics» in a region where the ring dispersion is zero. Therefore, all elements of the short bunch operation system should be located in the straight sections. For this purpose one has to extend the straight sections to a total length of 4 m in order to accommodate both the phase compressor and decompressor.

The amplitude of the debuncher voltage can be estimated from the expression

$$V = \frac{\delta E}{\sin(\Delta\varphi)}, \quad (5)$$

where  $\Delta\varphi$  is again the phase advance from the time focus to the debuncher. Under the assumption that the phase debuncher is located at the end of the straight section and that the energy spread induced by the phase compressor is  $\Delta E = 250$  eV (100 eV), the phase advance from the middle of the straight section to the position of the energy compressor is  $45^\circ$  ( $18^\circ$ ). Thus, the required debuncher RF voltage is within the range of  $V = 250/\sin(45^\circ) = 350$  V and  $V = 100/\sin(18^\circ) = 330$  V.

Due to energy spread  $\Delta E/E = 1.2\%$  imposed on the beam by the phase compressor, the pulses will be spread out from  $\tau \approx 2$  ns in the time focus to  $\tau \approx 7$  ns at the position of the debuncher. Assuming the conservation of the longitudinal emittance, the energy spread in the decompressed beam is reduced from 250 eV to roughly 70 eV, following (1):  $\Delta E = \varepsilon_{\text{lb}}/\Delta\tau = 500 \text{ eV} \cdot \text{ns} / 7 \text{ ns} = 70 \text{ eV}$ .

The residual energy spread during the passage of the buncher–debuncher chain is expected to be reduced from  $\Delta E/E = 1.2\%$  in the time focus to  $\Delta E/E = 3 \cdot 10^{-3}$  behind the energy compressor.

The bunches will then approach the 20 MHz RF cavity which might be located in the opposite straight section of the USR at a distance of  $L \approx 20$  m from the debuncher. For a rotation period of  $\sim 20 \mu\text{s}$  and a residual energy spread of  $3 \cdot 10^{-3}$ , the pulse width will grow from 7 ns (bunch half-width) to 23 ns. Since the dimension of each RF bucket is 50 ns (full separatrix), the bunches will be captured by the RF cavity for the next cycle without any beam losses.

It should be pointed out that our preliminary estimations do not include the beam behavior in the focusing elements of the ring. One clearly has to expect that the energy spread of the circulating beam will grow due to nonlinear effects in the phase compressor and decompressor. A next step will thus be to use advanced computer codes like, e.g., ESME to estimate the range of variation of the RF cavity voltage and the dynamic behavior of the beam in longitudinal phase space. In these simulations, we will also address the question of energy spread and required voltages on the RF cavity for higher harmonic modes.

**Choice of RF Cavity Parameters to Provide High Harmonic Mode.** As was stipulated in the previous section, the main RF cavity should provide adiabatic capture of the coasting beam into 50 ns buckets and adjust the time structure of the bunches, as well as the beam energy during short pulse operation mode. Following our simulations, the 20 MHz RF frequency range seems to be the ideal solution to obtain 1–2 ns short pulses.

The rotation period of antiprotons at  $E = 20$  keV in the USR ring is 18–22  $\mu$ s, see Table 1, with a revolution frequency of 46–56 kHz. One has to use high RF harmonic mode of operation ( $h_{\text{RF}} = 360$ –440) to split the coasting beam into 360–440 bunches.

The total bucket area for protons (all  $h_{\text{RF}}$  buckets) is [10]

$$A_{\text{It}} [\text{eV} \cdot \text{s}] = 16 \frac{R}{c} \alpha(\Gamma_s) \sqrt{\frac{eVE}{2\pi |\eta| h}}, \quad (6)$$

where  $R$  [m] is the machine radius;  $c$  [m/s] is the velocity of light;  $V$  is the peak RF voltage;  $h$  is the harmonic number,  $E$  [eV] =  $\gamma E_{0p}$  is the total energy ( $E_{0p}$  is the *proton* rest energy), and  $e$  is the elementary charge (equal to 1 when eV is used as energy unit);  $\alpha(\Gamma_s)$  is the moving bucket function ( $\Gamma_s = \sin \phi_s$ , where  $\phi_s$  is the synchronous phase angle), and  $\eta = 1/\gamma_t^2 - 1/\gamma^2$  is the frequency slip factor.

The area per bucket is  $1/h$  of the total area  $A_{\text{It}}$ :

$$A_{\text{It}} [\text{eV} \cdot \text{s}] = 16 \frac{R}{c} \alpha(\Gamma_s) \sqrt{\frac{eVE}{2\pi |\eta| h^3}} \quad (7)$$

and the moving bucket area function  $\alpha(\Gamma_s)$  can be approximated by a power series

$$\begin{aligned} \alpha(\Gamma_s) = & -4.869298085 \times \Gamma_s^7 + 21.563437656 \times \Gamma_s^6 - \\ & - 38.304144731 \times \Gamma_s^5 + 35.560953904 \times \Gamma_s^4 - 18.839475275 \times \Gamma_s^3 + \\ & + 6.323558981 \times \Gamma_s^2 - 2.435032449 \times \Gamma_s + 1. \quad (8) \end{aligned}$$

This function is plotted in Fig. 10 together with the moving bucket function obtained from numerical integration, as well as the error in percent. It can be seen from the graph that the error is less than 0.5% and that for most values of  $\Gamma_s$  the error is even less than 0.1%.

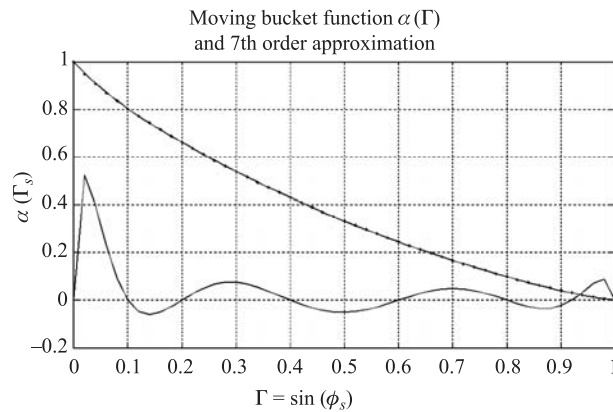


Fig. 10. Moving bucket function  $\alpha(\Gamma_s)$  and error in percent

For a partial filling of the bucket, the stationary bucket filling factor  $\alpha(\phi_L) = \varepsilon_{1b}/A_{1b}$ , where  $\varepsilon_{1b}$  is the longitudinal emittance per bunch and  $A_{1b}$  is bucket area, can be well approximated by

$$\alpha(\phi_L) = \frac{\pi\phi_L^2}{64} + \frac{(1 - \pi^3/16)\phi_L^4}{16\pi^4}, \quad (9)$$

where  $0 \leq \phi_L \leq 2\pi$  is the full bunch length in RF radians. The expression is exact in the limit of short bunches and for a full bucket, i.e.,  $\alpha(2\pi) = 1$ . For any intermediate value, the error does not exceed 0.5%.

The above equation can easily be solved for  $\phi_L$  and one can extract the full bunch length in radians as a function of the bucket filling:

$$\phi_L(\alpha) = \pi \sqrt{\frac{\pi^3/8 - \sqrt{\pi^6/64 - 16\alpha(\pi^3/16 - 1)}}{\pi^3/16 - 1}}. \quad (10)$$

The minimum voltage required to capture a bunch of an area  $\varepsilon_{1b}$  can then be derived from the general expression (2):

$$eV = \frac{\pi \varepsilon_{1b}^2 h^3 |\eta|}{128 (R/c)^2 \alpha^2 (\Gamma_s) E}. \quad (11)$$

The *full bunch* height for a stationary bucket is given by

$$\frac{\Delta p}{p} = \frac{2 \sin(\phi_L/4)}{\beta} \sqrt{\frac{2eV}{\pi h |\eta| E}}; \quad \frac{\Delta E}{E} = 2\beta \sin(\phi_L/4) \sqrt{\frac{2eV}{\pi h |\eta| E}}, \quad (12)$$

where  $\phi_L$  is the *full bunch* length in RF radians.

The *full bucket* height for a stationary bucket then follows directly from (12):

$$\frac{\Delta p}{p} = \frac{2}{\beta} \sqrt{\frac{2eV}{\pi h |\eta| E}}; \quad \frac{\Delta E}{E} = 2\beta \sqrt{\frac{2eV}{\pi h |\eta| E}}. \quad (13)$$

For moving buckets the *full bucket* height then becomes

$$\frac{\Delta p}{p} = \frac{2Y(\phi_s)}{\beta} \sqrt{\frac{eV}{\pi h |\eta| E} \frac{\zeta}{A_r}}; \quad \frac{\Delta E}{E} = 2Y(\phi_s) \beta \sqrt{\frac{eV}{\pi h |\eta| E} \frac{\zeta}{A_r}}, \quad (14)$$

where  $\xi$  is the ion's charge and  $A_r$  is its mass number. The filling factor parameter  $Y(\phi_s)$  is estimated from the expression

$$Y(\phi_s) = \sqrt{2 \cos \phi_s + (2\phi_s - \pi) \sin \phi_s}. \quad (15)$$

Finally the synchrotron frequency for protons is given by

$$f_{s0} = \frac{c}{2\pi R} \sqrt{\frac{h |\eta| eV \cos \phi_s}{2\pi E}}. \quad (16)$$

In the following, we will assume a synchrotron phase of  $\varphi_s \approx 0$  and a filling factor of  $\alpha(\sin \varphi_s) = 1$  for the USR.

Table 2. Coasting beam emittance and total bucket area for different energy spreads

| Initial energy spread $dE/E$ | Energy spread $dE$ , V | Coasting beam emittance, keV·ns | RF harmonic $h_{RF}$ | Infinity frequency, MHz | RF voltage, V | Total bucket area $A_{L\Sigma}$ , keV·ns |
|------------------------------|------------------------|---------------------------------|----------------------|-------------------------|---------------|--|
| $5 \cdot 10^{-4}$            | 10                     | 220                             | 440                  | 43.9                    | 0.8           | 220                                      |
| $10^{-3}$                    | 20                     | 440                             | 440                  | 43.9                    | 3.2           | 440                                      |
| $5 \cdot 10^{-3}$            | 100                    | 2200                            | 440                  | 43.9                    | 82            | 2200                                     |
| $10^{-2}$                    | 200                    | 4400                            | 440                  | 43.9                    | 343           | 4400                                     |
| $2 \cdot 10^{-2}$            | 400                    | 8800                            | 440                  | 43.9                    | 1370          | 8800                                     |
| $3 \cdot 10^{-2}$            | 600                    | 13200                           | 440                  | 43.9                    | 3084          | 13200                                    |
| $4 \cdot 10^{-2}$            | 800                    | 16000                           | 440                  | 43.9                    | 4530          | 16000                                    |

Table 3. Full bucket momentum and energy height

| $V_{RF}$ , eV | $dP/P = 4 \cdot 10^{-4} (V_{RF})^{1/2}$ | $2dE = 17(V_{RF})^{1/2}$ , eV | $E_k$ , keV | $2dE/E_k$           |
|---------------|---|-------------------------------|-------------|---------------------|
| 2             | $5.6 \cdot 10^{-4}$                     | 24                            | 20          | $10^{-3}$           |
| 10            | $1.2 \cdot 10^{-3}$                     | 54                            | 20          | $2.7 \cdot 10^{-3}$ |
| 40            | $2.5 \cdot 10^{-3}$                     | 108                           | 20          | $5.3 \cdot 10^{-3}$ |
| 100           | $4 \cdot 10^{-3}$                       | 170                           | 20          | $8.5 \cdot 10^{-3}$ |
| 200           | $5.6 \cdot 10^{-3}$                     | 240                           | 20          | $1.2 \cdot 10^{-2}$ |
| 500           | $9 \cdot 10^{-3}$                       | 380                           | 20          | $1.9 \cdot 10^{-2}$ |
| 1000          | $1.3 \cdot 10^{-2}$                     | 540                           | 20          | $2.7 \cdot 10^{-2}$ |
| 2500          | $2 \cdot 10^{-2}$                       | 850                           | 20          | $4.2 \cdot 10^{-2}$ |

The longitudinal emittance of the coasting beam, the total bucket area and the required amplitude of the RF voltage for the USR short pulse operation mode depend on the initial energy spread of the cooled beam and are provided in Table 2.

The growth in energy spread during the pulsed operation mode has to be carefully calculated. To avoid beam losses, the bucket area must follow the growing beam emittance. For that purpose, one has to provide a dynamic increase of the RF voltage amplitude in phase with the increasing beam emittance. The dynamic range of the RF cavity should then cover variations of the voltage amplitude from 2 V to roughly 2 kV.

The full bucket height (momentum  $dP/P$  and energy spread  $2dE/E_k$ ) for the stationary case is defined by (13), with some examples shown in Table 3.

In order to provide isoadiabatic conditions, the RF voltage should grow reasonably slow; for one period of the synchrotron oscillation the amplitude of the RF voltage might be increased by no more than 50%. This assures a constant degree of adiabaticity. Simulations show that in this case the process is reasonably adiabatic, while for higher values significant blowup and beam filamentation occurs.

The rotation frequency of 20 keV ions in the USR is about 45 kHz. Its synchrotron frequency is proportional to  $\Omega_S = 1.707 \times (eV_{RF})^{1/2}$  and may be varied from 2 kHz, corresponding to 2 V, to 76 kHz, i.e., 2 kV. Thus, isoadiabatic conditions during the USR short pulse operation can probably not be expected and one should expect significant beam filamentation, as well as an increase of the effective emittance. It is thus mandatory to perform

a full-scale computer simulation with computer codes like, e.g., ESME to build up a complete model and thorough understanding of the USR ring short pulse operation mode.

### SUMMARY AND OUTLOOK

The future ultralow energy storage ring at the facility for low-energy antiproton and ion research will provide antiprotons and possibly highly charged ions with unprecedented beam quality and luminosities in the energy range of 300 down to 20 keV.

In-ring collision studies with a so-called reaction microscope are of particular importance since they directly address one of the most fundamental yet unanswered problems in physics — the few-body Coulomb problem and in particular the question whether or not correlation effects are important for a full understanding and possibly even control of this process.

For these experiments, shortest beam pulses in the range of 1–2 nanoseconds at lowest beam energies are necessary. Given the natural dispersion of the beam and the coupling between transverse and longitudinal motion in an electrostatic storage ring, such pulses are very difficult to realize. In this paper, we present the results of a preliminary study that was aimed at an estimation of a possible beam bunching scenario in the USR. The simulations indicate that even shortest pulses might be realizable if an adequate beam forming scheme is applied.

The next step will now be to extend these simulations and to build up a full bunch rotation model, where the beam dynamics in longitudinal and transverse phase space will be investigated in detail.

**Acknowledgements.** The generous support of the Helmholtz Association of National Research Centers (HGF) under contract number VH-NG-328 and of the Gesellschaft für Schwerionenforschung (GSI), Darmstadt, is acknowledged. The authors greatly appreciate the help and useful advice of Pavel Belochitskii (CERN).

### REFERENCES

1. *Welsch C.P. et al.* Layout of the USR at FLAIR // Proc. Eur. Part. Acc. Conf. Edinburgh, Scotland, 2006.
2. *Welsch C.P. et al.* An Ultra-Low-Energy Storage Ring at FLAIR // Nucl. Instr. Meth. A. 2005. V. 546. P. 405–417.
3. <http://www.oew.ac.at/smi/flair/TechnicalProposal/TP.htm>
4. *Welsch C.P., Ullrich J.* FLAIR — A Facility for Low-Energy Antiproton and Ion Research at GSI // Hyp. Int. 2007. V. 172(1–3). P. 71–80.
5. *Fischer D. et al.* GSI Sci. Rep. 2006.
6. *Welsch C.P. et al.* Exploring Sub-Femtosecond Correlated Dynamics with an Ultra-Low Energy Electrostatic Storage Ring // AIP Conf. Proc. 2005. V. 796. P. 266–271.
7. *Welsch C.P., Smirnov A.V.* Cooling Rates of the USR as Calculated with BETACOOOL // AIP Conf. Proc. 2006. V. 821. P. 397–401.

8. *Welsch C. P. et al.* Ultra-Low Energy Antiprotons at FLAIR // Proc. Eur. Part. Acc. Conf. Lucerne, Switzerland, 2004.
9. *Kalagin I.* Computer Code: Buncher U-400. JINR Techn. Rep. 2004.
10. *Beloshitsky P.* CERN private commun. 2007.

Received on March 29, 2008.